
Research article

Measurement and validation of polysilicon photovoltaic module degradation rates over five years of field exposure in Oman

Honnurvali Mohamed Shaik^{1,*}, Adnan Kabbani¹, Abdul Manan Sheikh¹, Keng Goh², Naren Gupta² and Tariq Umar³

¹ Department of Electronics and Communication, A'sharqiyah University, P.O. Box 42, Postal Code 400, Ibra, Sultanate of Oman

² School of Engineering and Built Environment, Edinburgh Napier University, Scotland, UK

³ Department of Architecture and the Built Environment, University of the West of England, Bristol, UK

* **Correspondence:** Email: honnur.vali420@gmail.com; Tel: +96825401193.

Abstract: Degradation of PV modules have a severe impact on its power-producing capabilities thus affecting the reliability, performance over the long run. To understand the PV degradation happening under the influence of local environmental conditions a survey was conducted on six polycrystalline silicon-based PV modules over five years. It has been observed that the average degradation rates stood at 1.02%/year at irradiances 800 W/m² and 0.99%/year at irradiances 600 W/m², which are almost double the manufacturer proposed values. Upon further investigations, it has been found that discoloration of encapsulant in modules 3, 5, and 6 have been the main factor causing the reduction of the short circuit current (I_{sc}) thus affecting the overall power production capacity of the installed PV system. Considering the amount of time, resources and manpower invested to perform this survey an alternate way of estimating the PV degradation rates is also investigated. The exponential decay factor-based model is adopted to correlate the encapsulant discoloration seen on-site in the form of a mathematical equation to predict the current loss. This loss is defined as the visual loss factor in this paper. Further, the output I-V curves are simulated using MATLAB Simulink-based mathematical model which also integrates visual loss factor (VLF) losses into it. Such simulated I-V curves have shown a good match with the measured I-V curves at the same irradiance with an error less than 3%. Authors anticipate that this modelling approach can open the door for further research in developing algorithms that can simulate the PV degradation rates.

Keywords: Photovoltaics; PV Degradation rate; Polysilicon; short circuit current; PV discoloration; visual loss factor; MATLAB; Standard test Conditions (STC)

Abbreviations: PV system: Photovoltaic system; PV module: Photovoltaic Module; STC: Standard Test Conditions; I-V & P-V: Current-Voltage & Power-Voltage; q : Charge of an electron = 1.602×10^{-19} C; K : Boltzmann's constant = 1.380×10^{-23} J/K; E_g : Forbidden Energy bandgap, for silicon = 1.1 eV; A (or) n : Ideality factor of the diode; N_s : Number of cells connected in series; N_p : Number of cells connected in parallel; T_0 : Real-time temperature [k]; T_r : Reference temperature [k]; I_{ph} : Photocurrent of a solar PV cell generated due to solar irradiation [A]; K_i : Temperature coefficient of Isc cell short circuit current; V_{oc} : Open circuit voltage [V]; I_{rs} : Diode reverse saturation current at real-time temperature [A]; R_s : Series resistance of the PV module [Ω]; R_p : Parallel resistance of the PV module [Ω]; I : Output current from the PV panel [A]; P_{max} : maximum output power [W]; P_m : Maximum power at STC[W]; V_{mp} : Maximum power voltage [V]; I_{mp} : Maximum power current [A]

1. Introduction

Sultanate of Oman, one of the countries in the GCC (Gulf Cooperation Council) member countries has set a vision to generate 15% (around 3GW) of the total energy production through renewable sources. Considering the local hot environmental conditions of Oman, solar and wind are identified as the best sources in harvesting the maximum energy [1] among the renewables. As of, the global PV installation capacity was around 386 GW in the year 2017 and was increased to 480 GW for the next year 2018 (20% increase with the preceding year). Similarly, it is raised to 594 GW by the end of the last year 2019 (20% increase). Considering the abundant resource availability and the cost-competitiveness, solar installation is expected to grow by six folds reaching an installed capacity of around 2840 GW by the next ten years (2030) [2]. Considering such huge investments being made in the PV industry, the accurate estimation of payback time/return on investments plays a crucial role for the stakeholders, researchers, and PV industry-related individuals. On the other hand, neglecting the PV degradation exhibited by such solar panels may likely cause an imbalance in the estimated return on investments with the actual field data. Sultanate of Oman is blessed with abundant irradiance (6.47–6.85 kWh/m²/day), long day duration (approx. 14–16 hrs./day in summer) with clear skies which are all favorable factors to deploy solar technology to generate energy. However, despite having the huge potential in generating energy through solar, there exist some challenges. Hot climatic conditions, dust, and high humidity at the coastal areas of the land spread are few to mention. As a result, there are many concerns from the stakeholders and investors regarding its performance over the long run. The long-term performance (which means at least, 10–20 years) of the PV systems has not been investigated in these environmental conditions. This is because the PV installations started to deploy in 2014 only and are currently being under investigation in terms of their reliability and performance over the long run. Similarly, degradation rates reported in different parts of the world including Oman are summarized in below Table 1.

Table 1. Summary of PV Degradation rates that were reported from different parts of the world.

PV Degradation rates	Region	Summary of the study
The average degradation rate determined for the best modules is 0.85%/year and 1.1%/year for all the modules.	USA [3] Tempe, Arizona (a hot dry desert climate).	The study was conducted to determine the PV degradation rates for 16 years old PV systems.
The average degradation rate determined for so-called “good modules” is 1.33%/year. Higher degradation rates were observed for modules that do not fall under the good modules category.	India [4] All over India with varying climatic zones.	All India survey was conducted on more than a thousand PV modules to understand their performance since their initial installation.
The average degradation rate seen is about 1.96%/year.	Oman [5] Muscat, Al-batinah & Ash Sharqiyah governorates. (hot, dry, and humid climatic conditions).	High degradation rates are due to hot & humid climatic conditions and also due to the type of PV installation.
The degradation rate observed is about 1.15%/year.	Korea [6] Chungbuk, South Korea (moderate climate).	This study has proposed a disposal algorithm to evaluate the time interval of the optimal replacement of PV modules.
The degradation rates observed is in between 0.8% to 1.1%/year.	Italy [7] Tuscany, Italy (Transitional Mediterranean).	This study shows how choosing arbitrary electric storage can optimize capacity and foster the performance of the PV system.
The degradation rate observed is 1.96%/year.	China [8] Shenzhen, China (hot-humid climatic conditions).	Monocrystalline modules installed over 18 years on-site have been studied to estimate the degradation rates. A decrease in the FF of the modules has caused an increase in the series resistance.
Polysilicon PV modules showed 1.46%/year degradation rates, CIGS modules with 3.9%/year and least were mono-crystalline silicon with 0.07%/year.	UAE [9] Dubai, UAE (Desert climatic conditions).	Degradation rates of more than 27 types of PV modules installed in desert climatic conditions of Dubai are reported using python based NREL/Rdtools.
An annual degradation rate of 0.26%/year is observed just within a year of its installation.	Saudi Arabia [10] Jeddah, Saudi Arabia (Desert Climatic conditions).	The performance of the 58 kWp PV system (installed in Jeddah) is analyzed. Root mean square error (RMSE) is observed at 2.94% for six big data analysis modules for output power prediction.

Continued on next page

PV Degradation rates	Region	Summary of the study
Degradation rates of about 1.7%/year and 3.6%/year are reported for field A operating for 10 years and field B operating for 5 years.	Algeria [11] Biskra, North of Algeria sahara (semi-arid type of climate).	Monocrystalline-silicon PV modules are investigated in two field regions (A & B). I-V curves are measured and translated to STC conditions to estimate the PV degradation rates.
Power degradation in terms of percentage is observed from 13% to 15% installed over 31 years.	Libya [12] Kufra, Libiya (Desert climatic conditions).	Multicrystalline PV modules installed in the Libyan desert climate were investigated. Both outdoor and indoor measurements were performed to understand the performance of the PV modules and found that their life expectancy can be increased to forty years.

Therefore, globally, almost all the PV modules are showing degradation due to various environmental and other socio-economic factors. However, the investigation of these degradation rates requires longtime, sophisticated types of equipment that tend to be costlier. Further, the simulation resources to estimate the PV degradation is so far very limited and are also dependent on on-site measurement data. Therefore, in this paper, an attempt is made to simulate PV degradation rates in contrast to the traditional methods. Such simulated PV degradation rates may help the stakeholders to estimate the likely behavior of the PV modules avoiding robust measurement techniques that further require human resources, time, and costly pieces of equipment. Mathematically modeling the failures seen on-site provides a good opportunity to analytically predict the PV performance over the years to come and thus can take proper actions with efficient management.

Estimation of photovoltaic degradation rates requires the knowledge of the initial performance of the PV modules at the time of the first installation. In this paper, six polycrystalline PV modules are considered to estimate the degradation rates. The initial installation has implemented during the year 2014 to meet the energy demands of a base transceiver station that supports the local telecom network. Since then, every year their performance is being monitored and inspected. Generally, factors affecting the PV module performance are front side delamination, hotspots formation, discoloration of the encapsulant, interconnect failures, etc. these factors either cause a decrease in the (I_{sc}) or open-circuit voltage (V_{oc}) further leading to the reduction of the maximum output power of a PV module. It is very crucial to determine the faulty panels (degrading panels) at the beginning stage, for a proper function of the whole implemented PV system [13]. The prime challenge in using simulation-based tools is, how well the simulated results predict real-time behavior? In our survey, three PV modules (PV modules 3, 5, and 6) have been observed with discoloration of the encapsulate which is causing the reduction of the I_{sc} thereby decreasing the maximum output power. A mathematical exponential decay factor equation to estimate the discoloration loss is developed based on the measurement data which is termed a visual loss factor (VLF). The total output PV current (I) equation is modified by incorporating this loss into it to be able to predict the amount of current loss caused due to the encapsulant discoloration. A Simulink model has been developed to simulate the I-V curves which include the modelled visual loss factor (VLF) equations. The results have shown good accuracy as

with the measured data. Further, the PV degradation rates of each module for five years are measured and compared with the developed simulation model to validate the model.

2. Estimation of PV degradation and experimental setup

2.1. Description of experimental setup and data acquisition

Six-polycrystalline silicon (SUNTECH 240 Wp) PV modules mounted on the Iron stand elevated from the ground are considered in this study. The tilt angle of the mounted panels is around 21° northwest concerning the reference axis of the iron stand. The intend of this PV system solution is to supply power to the base transceiver station (BTS) which is placed in support of the local telecom network (Omantel). Further, it is an off-grid solution with a system size of around 1.4 KW. The generated power is stored using a 24 V battery connected with the MPPT charge controller and inverter. The specifications of the PV modules at STC (standard test conditions) are presented in Table 2. The STC here represents the simulation lab environment which is an industry-standard to represent the performance of the PV modules that specifies an irradiance of 1000 W/m^2 , operating cell temperature at 25°C with an air mass 1.5 (AM 1.5) spectrum. However, the real-time operating conditions differ largely with the manufacturer STC. Therefore, IEC 60891 standard provides a methodology to translate the measured I-V at different irradiances and temperatures to STC. The correction procedure considered in this study is comprehensively discussed in our previous work under section II (B) [14]. The test bench setup to measure the I-V and P-V curves is presented in the Figure 1. “MECO 9018 BT” portable solar analyzer is used to measure the I-V and P-V curves of the PV modules. Apart from that, an irradiance meter, temperature sensor, current, and voltage sensors are used to record the corresponding values during the measurement. To measure direct normal irradiance (DNI) through Pyrheliometer equipment along with a shading Pyranometer to measure the diffuse horizontal irradiance (DHI) was installed in the weather station of meteorology and air navigation, Muscat, Oman. This measured data is used to estimate the average irradiance and temperature per month. The global horizontal irradiance (GHI) can be calculated by using the formula $\text{GHI} = \text{DNI} \times \cos(z) + \text{DHI} \text{ W/m}^2$. Where (z) is the zenith angle. The data measured from these devices are monitored hourly basis. The averaged solar irradiance and temperature per month observed over five years of study is presented in Figure 2.

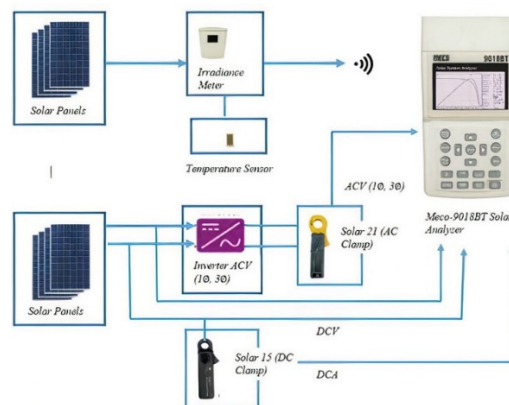


Figure 1. Test-bench setup to measure I-V curves.

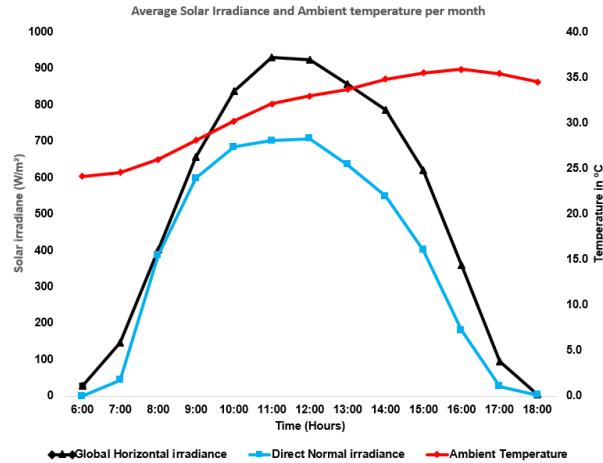


Figure 2. Averaged solar irradiance and ambient temperature per month.

Table 2. Suntech 240 W PV Panel Datasheet Specifications.

Parameters	Key Specifications
Max Power at STC (P_m)	240 W
Maximum power voltage (V_{mp})	30.2 V
Maximum power current (I_{mp})	7.95 A
Open circuit voltage (V_{oc})	37.2 V
Short circuit current (I_{sc})	8.43 A
No. of Cells in Series	60
No. of cells in parallel	1
Ideality factor (n)	1.2
Temperature coefficient of I_{sc} (K_i)	0.055%/°C
Reference Temperature	25 °C
Solar irradiance (W/m^2)	1000
PV technology type	Polycrystalline
Frame structure	Anodized aluminum alloy
Front Glass	3.2 mm (0.13 inches) tempered glass for extra protection of solar cells and EVA.
Solar Cell size & No. of cells	156 × 156 mm (6 inches) & 60 (6 × 10)
Cell encapsulation	EVA (Ethylene Vinyl Acetate)
Nominal Operating Cell Temperature (NOCT)	45 ± 2 °C

Wherein the peak irradiance is observed during the mid-noon hours (12:00–14:00). This also justifies that the recorded measurement readings are taken at the highest performance time of the PV modules. From Figure 2 one can notice that the daily average total GHI is 6646 Wh/m² averaged per month and DHI is 4914 Wh/m² averaged per month. This acknowledges that Oman has excellent solar energy potential. However, due to high average ambient temperatures (31.2 °C presented on the secondary axis of Figure 2), the PV module's performance would not be the same as the performance at Standard test conditions (25 °C).

2.2. Research methodology

The environmental conditions in the Sultanate of Oman usually remain hot and dusty (due to desert climate) for most of the year. Deposition and accumulation of dust particles affect the performance of the PV cell significantly. Research studies conducted by [15] have noted that the high wind speeds cause high dust accumulations leading to a sharp performance drop. However, the light transmittance was higher in the dust layer formed due to high wind speeds rather than the dust layer formed due to low wind speeds. This was mainly because of the dust sediment structure on the PV cell. Depending on the diameter size and deposition rate (g/m^2) of dust particulates the performance of the PV cell varies. The research study [16] noted that the fine particles (cement, carbon particulates) have severe detrimental effects than the coarser particles. Further, the study also noted that the performance of the PV cell is not correlated directly to the exposure time in the atmosphere for a given site rather it is the physical properties of the dust that determines the impact on the PV cell performance. Moreover, the research study [17] conducted in a laboratory simulating mars environmental dust conditions has also noted the reduction of the I_{sc} due to increased reflectance and decreased absorption at the visible light spectrum. Reduction of V_{oc} (caused by structural damage) is also noted in limited cases however, cleaning of PV cells has shown an increase back in the short-circuit current but was irreversible in the case of open-circuit voltage. Before performing measurements, PV modules were cleaned with water and sodium detergent to remove the dust accumulation. The impact of dust particles is not considered in our study as it falls out of the scope of our research study. Other researchers from Oman [18,19] have noted that the power reduction can go up to 60% depending on the dust particles size and if not cleaned for a month. Therefore, generally, PV sites have maintenance contracts with the suppliers for regular inspection, cleaning, and health monitoring of the PV modules. After cleaning the dust on the PV modules, they are short-circuited for about five minutes and thermally inspected by using an infrared camera to detect any hotspots formation or any faulty cell in the PV module. The next step is to record the I-V and P-V curves for each PV module at two different irradiances; one at mid-noon whose irradiance is around $800 \text{ W}/\text{m}^2$ and another at post noon whose irradiance is around $600 \text{ W}/\text{m}^2$. ‘Photovoltaic degradation’ is a mechanism where there is a reduction of PV output power gradually over time or due to any fault in the solar cells of the PV module. Factors causing PV degradation are mainly influenced by local environmental conditions, quality, installation type, etc. [20]. However, the major contributing factors arise from the local environmental conditions which vary from region to region across the globe. Oman experiences the desert type of climatic conditions, the factors affecting the degradation rates in such desert climatic conditions are comprehensively discussed in the literature [21]. PV degradation rate is calculated by Eq (1) as given below:

$$[P_{max} \text{ Degradation rate} = \frac{P_{max}(\text{initial value}) - P_{max}(\text{final value})}{P_{max}(\text{initial value}) \times \text{Age of the module}} \text{ \%/year}] \quad (1)$$

where P_{max} initial value is the maximum output power measured from the I-V curve during the first installation during the year 2014 and P_{max} final value is the maximum output power measured from the I-V curve after one year at least.

3. Modeling and simulation of i-v curves with vlf

One of the main limitations of doing on-site experimentation is the requirement of manpower,

lengthy time, and sophisticated costly equipment. Regarding it, stakeholders have requested if there could be any potential simulation tool that can approximate the PV degradation rates over time. Although there are various software's that can estimate the PV outpower based on the PV module specifications but are limited to STC and manufacturer set degradation values. They do not have an option to consider the actual on-site effects observed on-site and the ability to integrate into it. Therefore, authors have tried to mathematically model the encapsulant discoloration effect see on-site into equations that predict the reduction in the I_{sc} concerning the STC I-V and P-V curves. Thus, making the simulation model a good approximation to the real-time behavior of the PV system on site. In our study, Matlab Simulink is used to simulate the I-V curves of a PV module. A step-by-step procedure on how to build the model is very well comprehensively discussed in the literature [22]. This model is taken as a reference to build our model which is also based on one diode model. However, simulating the I-V curves at various irradiances and temperatures is not the main objective of this study. The main research challenge is to integrate the modelled equations (reduction in the short circuit current I_{sc} due to encapsulant discoloration) into the Simulink build and observe the I-V curves. Several other studies have been reported [23,24] considering Matlab and Simulink for modelling the PV cell, panel, and found to be a good match between the simulated and the experimental results. However, those studies did not include physical defects (discoloration of the encapsulant) factors that commonly play a vital role in the degradation of the PV module. A single diode model is considered in this study as shown in Figure 3.

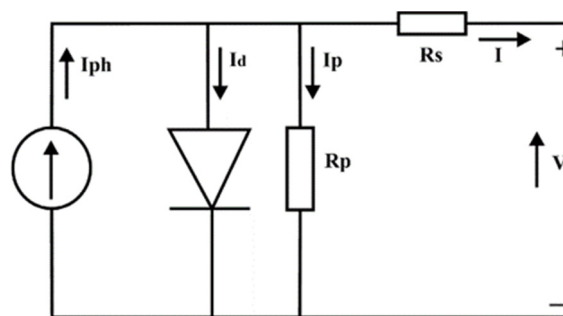


Figure 3. Single diode model of a PV cell.

Each solar cell in a PV module is modelled by the five parameters single diode model. R_s is the series resistance in the path of the current, which occurs mainly due to metal contacts, semi-conductor materials, connecting bus tracks. On the other hand, R_p is the parallel resistances that occur due to cell thickness and surface effects. The effect of R_p is more prominent only when the number of PV modules considered in the PV system is large [25]. Therefore, R_s has been taken into consideration while R_p is infinite. The output current I_{PV} of a solar cell is given by Eq (2) and the modified equation after considering R_p as infinite is given in Eq (3).

$$[I_{PV} = I_{Ph} - I_s \left[\exp \left(\frac{q(V+IR_s)}{N_s K A T_o} \right) - 1 \right] - \frac{V_p + IR_s}{R_p}] \quad (2)$$

$$[I_{PV} = I_{Ph} - I_s \left[\exp \left(\frac{q(V+IR_s)}{N_s K A T_o} \right) - 1 \right]] \quad (3)$$

As the PV module consists of solar cells connected in a series-parallel manner, the final output current I_{PV} of a PV module is given by Eq (4)

$$[I_{PV} = N_P \times I_{Ph} - N_P \times I_s \left[\exp \left(\frac{q(V+IR_s)}{N_s k A T_0} \right) - 1 \right]] \quad (4)$$

where, I_{ph} is the Photocurrent of a solar PV cell generated due to solar irradiation, I_s is the saturation current, V is the output voltage from the PV panel, q is the charge of an electron, k is Boltzmann's constant, A is the ideality factor of the diode, T_0 real-time temperature, N_s is the number of cells connected in series, I is the output current from the PV Panel, R_s is the series resistance of the PV panel and R_p is the parallel resistance of the PV panel. To compute the above equations, I_{ph} , I_{rs} and I_s are required which are given by Eqs (5), (6) and (7).

$$[I_{Ph} = [I_{sc} + K_i(T_0 - T_r)] \times \frac{G}{G_{ref}}] \quad (5)$$

$$[I_{rs} = I_{sc} / \left[\exp \left(\frac{qV_{oc}}{N_s k A T_0} \right) - 1 \right]] \quad (6)$$

$$[I_s = I_{rs} \left[\frac{T_0}{T_r} \right]^3 \exp \left[\left(\frac{qE_g}{Ak} \right) \left(\frac{1}{T_r} - \frac{1}{T_0} \right) \right]] \quad (7)$$

where K_i is the temperature coefficient of I_{sc} of the cell, I_{sc} is the short circuit current at STC, T_r is the reference temperature at STC, G is the measured solar irradiance, G_{ref} is the solar irradiance at STC, V_{oc} is the open-circuit voltage of the PV panel, I_{rs} is the diode reverse saturation current, E_g is the energy bandgap for the silicon (1.1 eV). To validate the encapsulant discoloration losses observed on-site from the measured data, the reduction in the short circuit current (I_{sc}) needs to be estimated first. The measured I-V curves during the initial year are compared with the manufacturer's I-V curves under STC. This reduction is obtained in a ratio form by comparing the measured I_{sc} to I_{sc} at STC and is defined by ILF (Short circuit current (I_{sc}) loss factor) and is given by Eq (8).

$$[ILF = \frac{I_{sc} \text{ measured at irradiance}}{I_{sc} \text{ at that irradiance under STC}}] \quad (8)$$

Further, to match the measured data we consider exponential decay factor ($e^{-0.625}$) to limit the current reduction ratio which is between 0.4 and 1. A detailed discussion of this model is presented in the next section. Now, the final equation called visual loss factor (VLF) which describes the measured encapsulant discoloration losses seen on site is given by Eq (9) as below:

$$[VLF = e^{-0.625 \times (ILF)}] \quad (9)$$

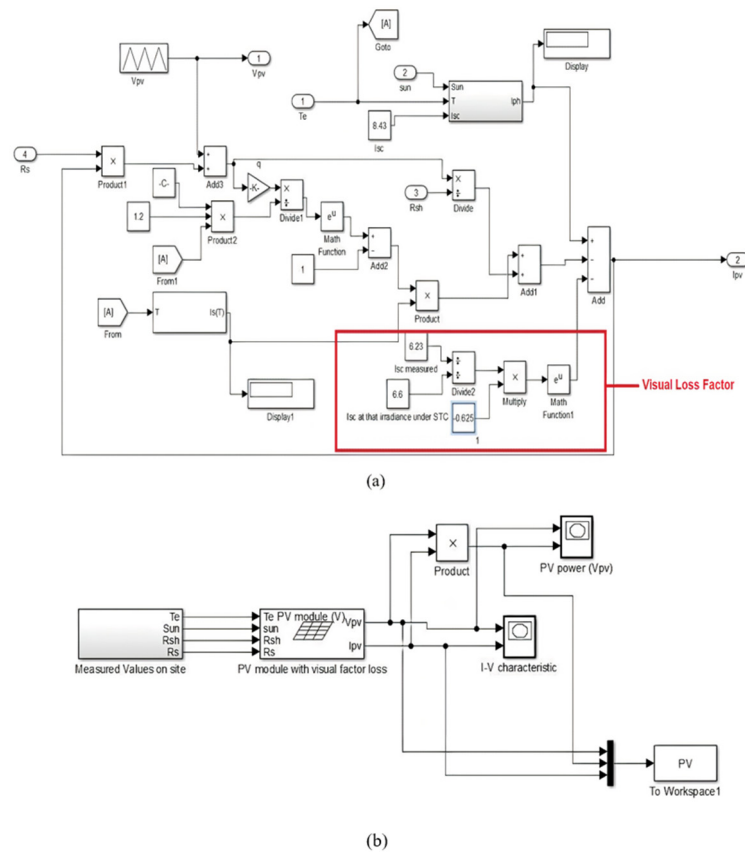


Figure 4. Simulink model to estimate the I-V and P-V curves with VLF. (a) Simulation of output current I_{PV} with VLF (subsystem); (b) Full system model to estimate the I-V and P-V curves.

Finally, the actual PV output current is estimated by subtracting the VLF losses from Eq (4) and is given by Eq (10) as below:

$$[I = [N_p \times I_{ph} - N_p \times I_s \left[\exp \left(\frac{q(V + IR_s)}{N_s K A T_o} \right) - 1 \right] - [e^{-0.625 \times (ILF)}]] \quad (10)$$

The entire simulation setup of this sub-system is presented in Figure 4a and the complete system which simulates the I-V and P-V curves is presented in Figure 4b to validate the consistency of Eq (8) two more Eqs (11) and (12) are also modelled with different exponential decay multiplication factors and are shown below:

$$[VLF = e^{-0.425 \times (ILF)}] \quad (11)$$

$$[VLF = e^{-0.125 \times (ILF)}] \quad (12)$$

The above two equations have shown good matching results when the measured irradiances were below 500 W/m^2 . However, for the solar irradiances above 600 W/m^2 the mismatch error percentage was above 25%. As a result, Eq (10) has been adopted in our simulation studies and the results are discussed in the next section.

4. Results and discussion

The site consists of six PV modules which will be termed as PV modules 1,2,3...6 in this paper. Table 3 shows the maximum output power (P_{\max}) of the measured P-V curves each year since 2014. Considering the initial installation year (2014), the average degradation rate for the six modules under the irradiance 800 W/m^2 is observed to be at $1.02\%/year$. while with irradiance 600 W/m^2 , the degradation rate seen is $0.99\%/year$. The measured average degradation error difference between the two irradiances is around 4% which is in the acceptable range. The observed degradation rates from our site PV modules seem to be higher than the degradation rates seen in other countries [26,27]. The reason is mainly due to discoloration of the encapsulant seen in modules 3, 5 and 6. Discoloration of the encapsulant causes the reduction in the I_{sc} thus decreasing the P_{\max} . Figure 5(a) shows PV Module 5 with browning effects observed on some of the PV cells. Figure 5(b) shows the Electroluminescence (EL) image of PV module 5 and Figure 5(c) shows the Infra-red (IR) image for PV module 5. To capture the EL images, an electroluminescence camera with a si-CCD (Charge-coupled device) sensor was used. The PV modules are forward biased using a DC power supply twice the rating of the short-circuit current. One can observe from Figure 5(a) that some of the cells are exhibiting the browning color which is light brown. Dark browning or yellowing of the encapsulate has not been observed yet. This can be correlated with the EL image presented in Figure 5(b). Dark portions are observed on the cells where browning of the encapsulate is prevalent. On the other hand, the corrosion effect is also noticed on one of the interconnects (highlighted in red color). Thermal imaging of the PV modules can help to detect the hotspots, cracks, etc. because the occurrence of hotspots or cracks on the PV cells tends to increase the temperature higher than their surrounding cells. From Figure 5(c), it can be observed that no such mismatch cell temperatures are found. All cell temperatures are found to be in normal operating conditions thus validating the absence of hotspots or cracks in the solar cells. Measured PV electrical parameters at STC during the initial and final years of measurement are presented in Table 4. All the electrical parameters are showing degradation when compared to the initial year of the measurement except R_s which is showing an increasing pattern. Furthermore, Figure 6 presents the degradation analysis of all the electrical parameters. It can be observed from Figure 6, that V_{oc} for all the six modules has seen little to no degradation over operating years thus remaining at the reference line in Figure 6. I_{sc} degradation for PV modules 3, 5, and 6 was higher ($\sim -1.4\%$) than the rest of the PV modules ($< -1\%$). P_{\max} has also shown higher degradation rates ($\sim > 5\%$) for PV modules 1, 3, 5, and 6 than the remaining modules ($< 5\%$). A similar decreasing trend can be observed for Fill Factor (FF) and Shunt resistance (R_{sh}). The degradation rates for FF are between -2% to -8% , while for R_{sh} the degradation rates are between -11% to -15% . On the other hand, series resistance (R_s) has been observed with positive degradation rates because of the increase in the series resistance value over the operated years. Furthermore, Figure 7 shows a sample of encapsulant discoloration observed on a cell in PV module 5. To validate the encapsulant discoloration ultraviolet-fluorescence (UVf) imaging is performed on one of the PV cells from PV module 5. The PV cell is cut into four regions and is termed as mini-cell 1 to 4 in this paper. Further, each mini-cell is connected to the controlled DC power source to observe the I-V characteristics. All minicells were placed over a 10 cm thick wool and glass insulation and tightly packed with aluminum foil. One light array (20 lamps) of UV lamps (380–390 nm) are placed with an angle of 48° with respect to the minicells surface to minimize glaring in the visual images. The observed UVf images at 800 kWh/m^2 UV dosage for all the minicells are presented in Figure 8(a). One can observe from the figure that light discoloration has been started in minicell 1

and 2. Similarly the change in yellowness index (ΔYI) taken by calorimeter for all the minicells are reported in Figure 8b. Figure 8b presents the yellow index for all the minicells during initial installation and after five years of field exposure. It can be observed that minicell 1 and minicell 2 have shown a higher change in yellowness index when compared to minicell 3 and 4 after five years of field exposure. Similarly increase in the UV dosage has resulted in a higher change in the yellowness index. This confirms that the EVA is absorbing the UV rays causing the material to degrade faster. A recent research study conducted by Ja Eun Kim et al. [28] has noted that absorption of the UV rays into the UV-cut (UVC) EVA has accelerated the discoloration at a higher rate for higher UV dosages. The research study [29] on a 25 years old PV module has investigated the effects of discoloration of encapsulant and delamination on electrical parameters. It is observed that the output power has dropped by 18% due to a decrease in the short circuit current (I_{sc}). Another research study [30] has shown that the effect of high temperature and humidity causes the loss of adhesive properties due to which the performance of the PV module drops. The site location is not only influenced by the hot climate but also influenced by the high humidity levels due to its presence close to the seashore. Generally, humidity gets evaporated when the day starts to become hot, leaving the saline white formations on the front or back of the PV glass panel. Therefore, regular maintenance is recommended for the efficient performance of the PV panels. The salinity levels of the Arabian Gulf and Gulf of Oman and their potential influence on the PV module are discussed in our recent paper [31].

Table 3. Measured P_{max} on site for each PV module and their average degradation rates per year.

PV module sample	Measured Irradiance W/m^2	Year						Pmax degradation rate per year (in %)
		2014 (Pmax) in W (initial)	2015 (Pmax) in W	2016 (Pmax) in W	2017 (Pmax) in W	2018 (Pmax) in W	2019 (Pmax) in W (Final)	
Module 1	800	170	169	168	166	164	162.5	0.89
	600	140	139	138	137	136	134	0.85
Module 2	800	172	171	170	168	166	164	0.93
	600	146	145	143	141	140	139	0.95
Module 3	800	168	167	165	164	161	159	1.07
	600	145	143	141	140	139	137	1.10
Module 4	800	162	161	160	159	157	154	0.98
	600	142	141	140	138	137	135	0.98
Module 5	800	189	188	186	184	180	178	1.16
	600	150	149	148	147	145	142	1.06
Module 6	800	180	178	177	175	173	170	1.1
	600	152	152	151	149	147	144	1.05
Average degradation for six modules	800							1.02
	600							0.99

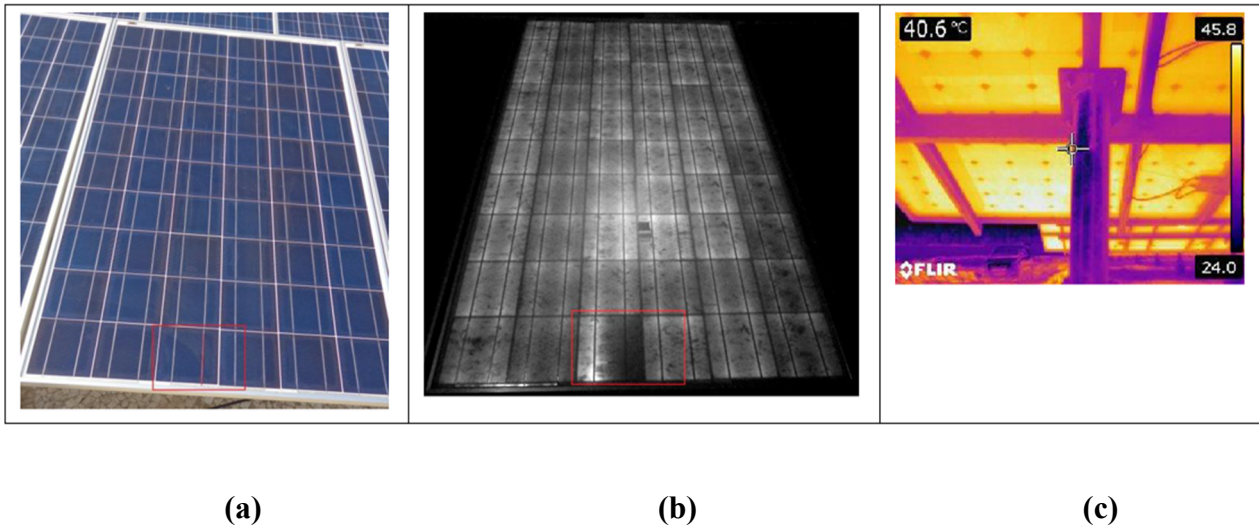


Figure 5. (a) Full view of PV Module 5; (b) EL Image of PV Module 5; (c) IR Image of PV Module 5.

Table 4. Measured PV Electrical Parameters during initial and final year at STC.

PV module sample	Year of measurement (Initial-2014 Final-2019)	PV Electrical Parameters					
		(P_{max}) in W	(I_{sc}) In A	(V_{oc}) In V	(FF) In %	R_s In Ω	R_{sh} In Ω
Module 1	Initial	174	6.96	34.2	73.1	1.6	66
	Final	165	6.9	33.6	71.4	2.1	58
Module 2	Initial	176	6.82	33.8	76.3	1.5	64
	Final	168	6.76	33.8	73.5	2	54
Module 3	Initial	170	6.86	34.0	72.8	1.4	65
	Final	161	6.76	33.8	70.4	2.2	56
Module 4	Initial	164	6.78	33.6	71.9	1.3	62
	Final	158	6.72	33.6	70	1.8	54
Module 5	Initial	194	6.84	34.1	83.1	1.1	72
	Final	174	6.74	34	76	1.8	61
Module 6	Initial	184	6.64	33.9	81.7	1.2	68
	Final	174	6.56	33.8	78.4	1.8	60

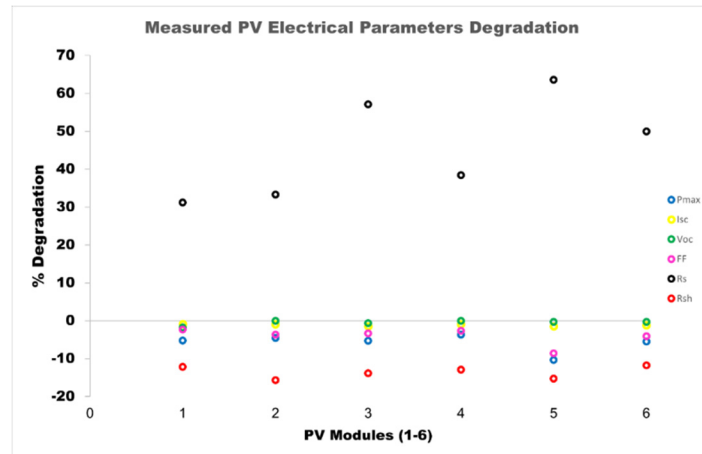


Figure 6. PV electrical parameters degradation.

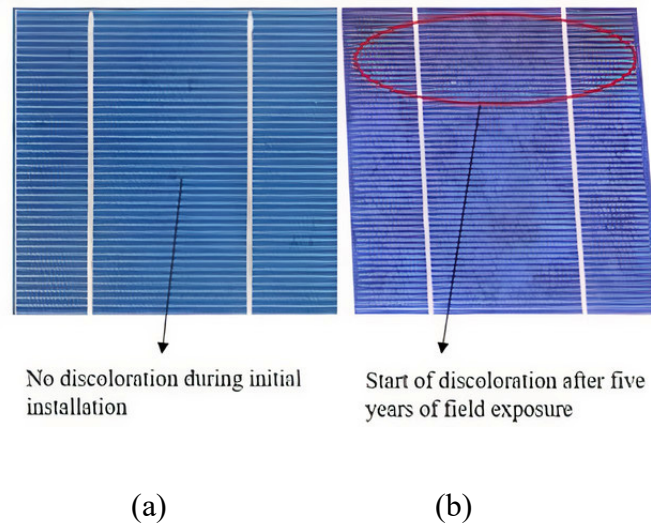


Figure 7. Module 5 PV cell from the site. (a) During the initial installation, module 5 PV cell shows no discoloration in the encapsulant; (b) After five years of field exposure, the top corner of the PV cell starts to brown.

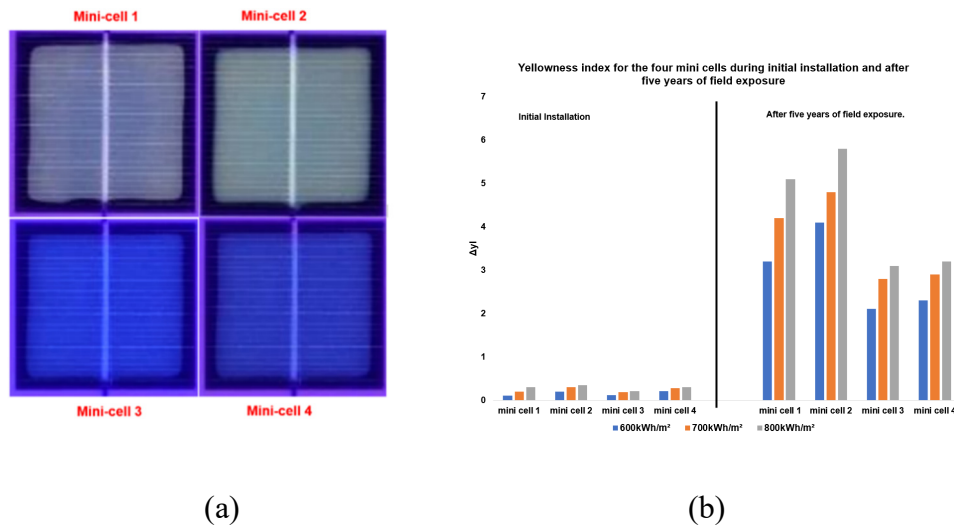


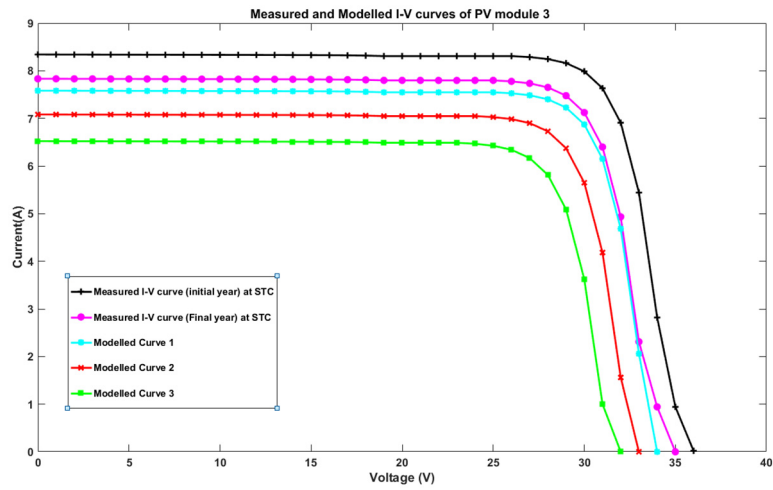
Figure 8. PV cell UVf and change in its yellowness index. (a) UVf images of the PV cell from PV module 5 at 800kWh/m² UV dosage; (b) Change in Yellowness index (ΔYI).

Among the surveyed six modules, modules 3, 5, and 6 have observed encapsulant discoloration due to which output current (I) of a PV module is decreased also leading to the reduction of maximum total output power (since $P_{\max} = V_{\text{mp}} \times I_{\text{mp}}$). As discussed in section 3, this loss in the current (I) is modelled by the mathematical Eqs (8), (9), (11) and (12). The basis of this modelling is done, considering the fact that the reduction of the output current is a natural decay phenomenon which happens gradually over time but not an instant phenomenon. Therefore, negative exponential decay (e^{-x}) factor is considered in our studies. The next question that arises is what should be ' x ' value? The ' x ' value in our studies is nothing but the decrease of the output current (I) due to encapsulant discoloration. This decrease in the current (I) is estimated by ILF (Eq (9)). For instance, consider the PV module 5, The measured I_{sc} (at MPPT point) at irradiance 800 W/m² was 5.8 A. On the other hand, The I_{sc} at the same irradiance under STC is approximated to 6.6 A from the datasheet [32]. Therefore, the ILF ratio value is 0.87 of the maximum current (6.6 A) it is supposed to be. On performing a similar analysis for all the rest of the PV modules we found the limit of the reduction ratio is between 0.4 to a maximum of 1. Where 0.4 indicates the highest decrease in the current I and 1 value indicates no decrease in the measured current with respect to the STC values given by the manufacturer. Therefore, the exponential ' x ' value should be in between the range $[0-1]$, i.e., ($e^{-0} = 1$ and $e^{-1} = 0.4$). Upon further testing multiplying by a factor 0.625 has shown better approximation to the measured values for irradiances above 600 W/m², 0.425 for the irradiances between 600 to 500 W/m², and 0.125 for the irradiances less than 500 W/m². Since our interest area of study is only on those I-V curves where the measurements were taken at least when the solar irradiance is above 600 W/m². A research study [33] conducted in India to estimate the PV degradation rates noted that the I-V curves recorded under irradiance 500 W/m² cannot be included in the degradation studies as the PV modules are not functioning at least 50% of their maximum performance and hence the obtained data is not reliable. The analysis of the ILF, VLF values, and modelled current values for PV modules 3, 5, and 6 after five years of field exposure under MPPT conditions is presented in Table 5.

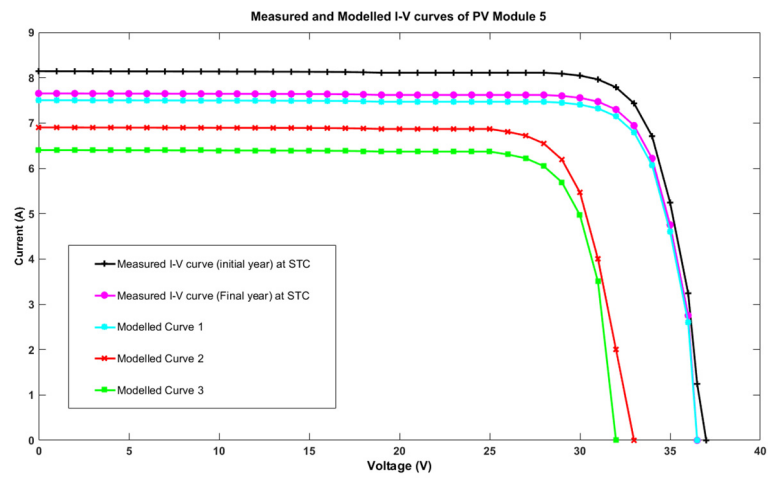
Table 5. ILF, VLF, and Modelled I_{sc} current values for PV modules 3, 5, and 6.

Parameters	PV Module 3	PV Module 5	PV Modules 6
Measured I_{sc} at irradiance 800 W/m^2	5.3 A	5.8 A	5.85
Manufacturer I_{sc} value at STC from data sheet	6.6 A	6.6 A	6.6 A
ILF (Eq (9))	0.8	0.87	0.88
VLF modelled equation (Eq (8))	0.6	0.57	0.57
Modelled current I_{sc} at irradiance 800 W/m^2 (Eq (10))	5.22 A	5.72 A	5.75 A

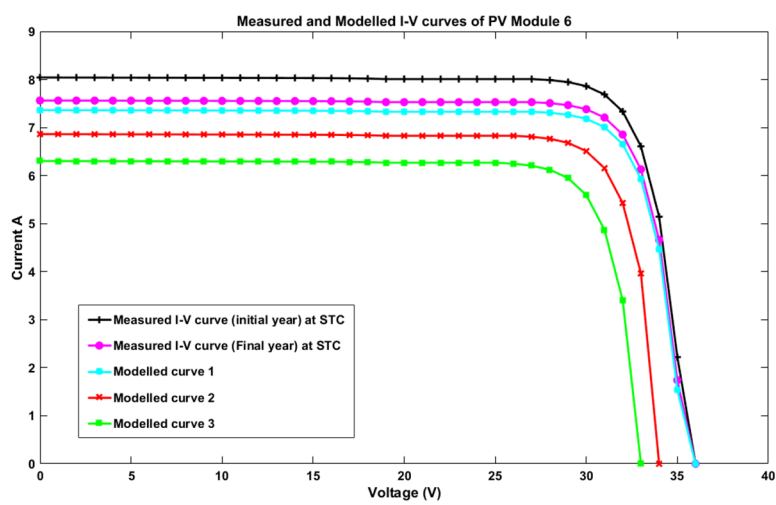
On the other hand, A sweep up to the open-circuit voltage (V_{oc}) is simulated for modules 3, 5, and 6. These modules have outlasted the manufacturer's degradation rates (i.e., more than 1%/year). The I-V curves for the three modules 3, 5, and 6 measured during the initial installation year (i.e., 2014) and after five years of field exposure along with the simulated I-V curves are presented in the Figure 9a,b,c. One can observe from Figure 9a,b,c, that the modelled curve 1 (which represents Eq (10)) has remained closer to the measured values after five years of field exposure. The modelled curve (2) and (3) representing Eq (10) but with VLF Eq (11) and (12). Their predictions have an average error percentage of about 14.6 and 29.2 from the measured values. For instance, consider PV module 3 I-V curves from Figure 9(a). The measured I_{mp} after 5 years of field exposure is 7.6 A (reference value) and the simulated I_{mp} from the modelled curve 1 is around 7.4 A whose error is 2.6%. On the other hand, the I_{mp} of modelled curve 2 is around 6.8 A resulting in a 10.5% error. Likewise, the I_{mp} of modelled curve 3 is around 6 A resulting in a 21% error. Performing similar calculations to all the modules and averaging the error values have observed an average error prediction rate of 14.6% for modelled curve 2 simulated I-V curves and 29.2% for modelled curve 3 simulated I-V curves. The maximum output power for the PV module 5 during the initial installation is 189 W and after five years of field exposure, the observed maximum output power is 178 W which is showing the average degradation rate of 1.16%/year (using Eq (1) and data from Table 3). Similarly, PV modules 3 and 6 have also shown higher degradation rates of more than 1%/year. According to the manufacturer warranty, the PV module degradation should not be crossing more than 0.5%/year. The current degradation rate is almost double the manufacturer data which raises concerns about its performance over the long run. Likewise, the observed degradation rates are 20% lower than UAE reported degradation rates [9] and almost similar to the USA reported degradation rates [3]. On the other hand, the developed Simulink model has shown good accuracy in estimating the decrease in I_{sc} due to encapsulant discoloration. The PV degradation rates for all the sample modules based year-wise are shown in the Figure 10. One can observe from the Figure 10 that the degradation rate for module 1 is the only PV module (for the first three years) that has remained within the manufacturer's specified level. The remaining modules have maintained the degradation rates higher than the specified level from the initial stages of the installation. PV Module 3, 5, and 6 have observed the highest degradation rates, more than 1%/year during the five years of field exposure. However, PV module 5 has seen a degradation rate higher than 1%/year just after three years of installation due to the encapsulant discoloration. All the simulated I-V curves along with the modelled VLF (Eq (8)) have shown a good correlation with the measured I-V curves at irradiance 800 W/m^2 with an error percentage less than 3.



(a)



(b)



(c)

Figure 9. Measured and Modelled I-V curve of PV modules 3, 5, and 6.

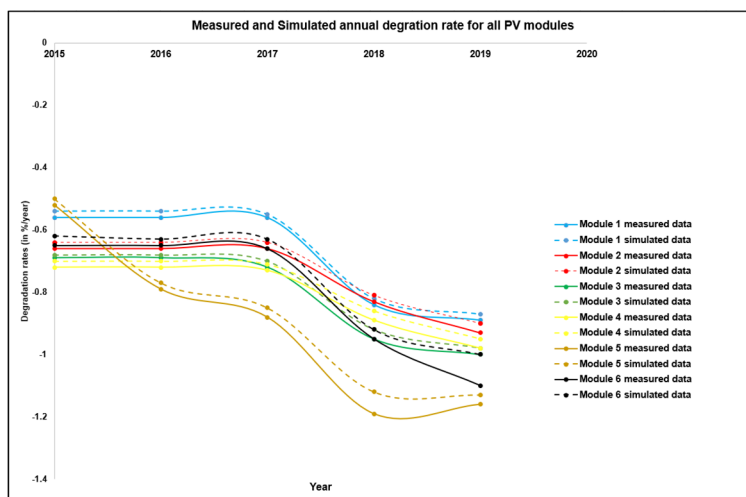


Figure 10. Measured and simulated annual degradation rate for all PV modules.

5. Conclusions

Understanding the performance of the PV modules subjected to field exposure plays a crucial role in improving system performance and in the decision-making process in future deployments. PV degradation rates for the six polycrystalline PV modules are calculated for a field exposure of five years in Oman. PV modules 1, 2, and 4 have been observed with degradation rates $<1\%/year$ and the rest of the PV modules higher than $1\%/year$. Overall, the results have shown higher degradation rates than the manufacturer proposed values. This is because of high temperatures and salty humid climate affecting the PV module encapsulant thereby causing the reduction in (I_{sc}) . Further, the analysis of electrical parameters has shown a negative degradation percentage of -5 to -10% for P_{max} , -0.8 to -1.46% for I_{sc} , 0 to -1.75% for V_{OC} , -2.3 to -8.54% for FF, -11.7 to -15.6% for R_{sh} except for R_s which has observed with positive degradation rates ranging from 31.2 to 63.6% . The change in yellowness index (ΔYI) for minicells 1 and 2 is between 5 to 6 (for 800 kWh/m^2 UV dosage) when compared with its initial installation yellowness index. Similarly, for minicells 3 and 4 it is in the range of 2 to 3 . This confirms the start of discoloration on the corners of the PV cell extending to the middle of the PV cell. Further, Visual loss factor equations are modelled and developed to incorporate the losses that occurred due to visual defects. The visual defects seen in our study are majorly encapsulant discoloration for three PV modules in which module 5 has observed light browning at the corners of some cells and in the middle for some cells. Similar light browning effects are also observed in PV modules 3 and 6. The total output current of the PV module is modified and simulated using Matlab to validate the measured data. The modelled curve 1 simulated result has shown a satisfactory match with an average error percentage of less than 3 . On the other hand, modelled curve 2 and 3 simulated results have shown an averaged error percentage of 14.6 and 29.2 . This study has helped to develop and incorporate the visual losses observed on-site into the simulation model which has created an opportunity to estimate the PV degradation rates in realistic to the measured data. However, the development of modelled equations in this paper is based on on-site measurements. As a potential future work, considering ongoing advances in the field of Artificial intelligence and machine learning one can develop algorithms that can continuously track the health of PV modules using sensor data.

Acknowledgments

The authors show their heartfelt gratitude and are thankful for the technical assistance received from the OSS (Oman Solar system LLC) and Omantel SAOG companies for conducting this case study.

Conflict of interest

The authors declare no conflict of interest in this paper.

References

1. Kazem HA (2011) Renewable energy in Oman: Status and future prospects. *Renewable Sustainable Energy Rev* 15: 3465–3469.
2. IRENA (2019) Future of Solar Photovoltaic: Deployment, investment, technology, grid integration, and socio-economic aspects (A Global Energy Transformation: paper), International Renewable Energy Agency, Abu Dhabi. Available from: https://www.irena.org//media/Files/IRENA/Agency/Publication/2019/Nov/IRENA_Future_of_Solar_PV_2019.pdf.
3. Yedidi K, Tatapudi S, Mallineni J, et al. (2014) Failure and degradation modes and rates of PV modules in a hot-dry climate: Results after 16 years of field exposure. *In 2014 IEEE 40th Photovoltaic Specialist Conference (PVSC), IEEE*, 3245–3247.
4. Dubey R, Chattopadhyay S, Kuthanazhi V, et al. (2017) Comprehensive study of performance degradation of field-mounted photovoltaic modules in India. *Energy Sci Eng* 5: 51–64.
5. Honnurvali MS, Gupta N, Goh K, et al. (2018) Case study of PV output power degradation rates in Oman. *IET Renewable Power Gener* 13: 352–360.
6. Park JH, Lee HD, Tae DH, et al. (2019) A study on disposal diagnosis algorithm of pv modules considering performance degradation rate. *J Korea Academia-Industrial Coop Soc* 20: 493–502.
7. Lovati M, Salvalai G, Fratus G, et al. (2019) New method for the early design of BIPV with electric storage: A case study in northern Italy. *Sustainable Cities Soc* 48: 101400.
8. Han H, Dong X, Lai H, et al. (2018) Analysis of the degradation of monocrystalline silicon photovoltaic modules after long-term exposure for 18 years in a hot–humid climate in China. *IEEE J Photovoltaics* 8: 806–812.
9. John JJ, Alnuaimi A, Elnosh A, et al. (2018) Estimating degradation rates from 27 different PV modules installed in desert conditions using the NREL/Rdtools. *In 2018 IEEE 7th World Conference on Photovoltaic Energy Conversion (WCPEC)(A Joint Conference of 45th IEEE PVSC, 28th PVSEC & 34th EU PVSEC) IEEE*, 712–714.
10. Oh W, Kang S, Chan SI (2017) Performance analysis of photovoltaic power system in Saudi Arabia. *J Korean Sol Energy Soc* 37: 81–90.
11. Charrouf O, Betka A, hadef H, et al. (2017) Degradation evaluation of PV modules operating under Northern Saharan environment in Algeria. *In AIP Conference Proceedings* 1814: 020030.
12. Alshushan MA, Saleh IM (2013) Power degradation and performance evaluation of PV modules after 31 years of work. *In 2013 IEEE 39th Photovoltaic Specialists Conference (PVSC)*, 2977–2982.
13. Hayashi T, Nagayama T, Tanaka T, et al. (2018) Influence of degradation in units of PV modules on electric power output of PV system. *J Int Counc Electr Eng* 8: 119–127.

14. Honnurvali MS, Gupta N (2017) PV electrical parameters degradation analysis-Oman perspective. *In 2017 8th International Renewable Energy Congress (IREC)*, 1–5.
15. Goossens D, Van Kerschaever E (1999) Aeolian dust deposition on photovoltaic solar cells: the effects of wind velocity and airborne dust concentration on cell performance. *Sol Energy* 66: 277–289.
16. El-Shobokshy MS, Hussein FM (1993) Effect of dust with different physical properties on the performance of photovoltaic cells. *Sol Energy* 51: 505–511.
17. McMillon-Brown L, Peshek TJ, Pal A, et al. (2021) A study of photovoltaic degradation modes due to dust interaction on Mars. *Sol Energy Mater Sol Cells* 221: 110880.
18. Kazem HA, Chaichan MT (2019) The effect of dust accumulation and cleaning methods on PV panels' outcomes based on an experimental study of six locations in Northern Oman. *Sol Energy* 187: 30–38.
19. Kazem HA, Chaichan MT (2016) Experimental analysis of the effect of dust's physical properties on photovoltaic modules in Northern Oman. *Sol Energy* 139: 68–80.
20. Jordan DC, Silverman TJ, Wohlgemuth JH, et al. (2017) Photovoltaic failure and degradation modes. *Prog Photovoltaics: Res Appl* 25: 318–326.
21. Kuitche JM, Pan R, TamizhMani G (2014) Investigation of dominant failure mode(s) for field-aged crystalline silicon PV modules under desert climatic conditions. *IEEE J Photovoltaics* 4: 814–826.
22. Zainal NA, Yusoff AR (2016) Modelling of photovoltaic module using matlab simulink. *In IOP Conference Series: Materials Science and Engineering* 114: 012137.
23. Hejri M, Mokhtari H, Azizian MR, et al. (2014) On the parameter extraction of a five-parameter double-diode model of photovoltaic cells and modules. *IEEE J Photovoltaics* 4: 915–923.
24. Siddique HAB, Xu P, De Doncker RW (2013) Parameter extraction algorithm for one-diode model of PV panels based on datasheet values. *In 2013 International Conference on Clean Electrical Power (ICCEP)*, 7–13.
25. Tina GM, Ventura C (2013) Evaluation and validation of an electrical model of photovoltaic module based on manufacturer measurement. *Sustainability in Energy and Buildings*, 15–24. Springer, Berlin, Heidelberg.
26. Sánchez-Friera P, Piliouline M, Pelaez J, et al. (2011) Analysis of degradation mechanisms of crystalline silicon PV modules after 12 years of operation in Southern Europe. *Prog Photovoltaics: Res Appl* 19: 658–666.
27. Jordan DC, Kurtz SR (2013) Photovoltaic degradation rates—an analytical review. *Prog Photovoltaics: Res Appl* 21: 12–29.
28. Kim J, Rabelo M, Padi SP, et al. (2021) A review of the degradation of photovoltaic modules for life expectancy. *Energies* 14: 4278.
29. Park NC, Jeong JS, Kang BJ, et al. (2013) The effect of encapsulant discoloration and delamination on the electrical characteristics of photovoltaic module. *Microelectron Reliab* 53: 1818–1822.
30. Badiee A, Ashcroft IA, Wildman RD (2016) The thermo-mechanical degradation of ethylene vinyl acetate used as a solar panel adhesive and encapsulant. *Int J Adhes Adhes* 68: 212–218.
31. Honnur Vali MS, Gupta N, Goh K, et al. (2020) Potential regions in the Persian Gulf to deploy offshore floating photovoltaic systems. *Proc Inst Civ Eng-Energy* 173: 94–100.

32. Suntech, 240Wp, polycrystalline solar PV module datasheet, Page 4; 2014; Available from: [https://esmediaproduct.s3.amazonaws.com/media/u/bad/9e9/d9b/4a377fac554a5266604e7b20285d4e78/Suntech%20STP%20230-260_20%20Wd\(poly\)_EN_web_1.pdf](https://esmediaproduct.s3.amazonaws.com/media/u/bad/9e9/d9b/4a377fac554a5266604e7b20285d4e78/Suntech%20STP%20230-260_20%20Wd(poly)_EN_web_1.pdf).
33. Golive YR, Zachariah S, Dubey R, et al. (2019) Analysis of field degradation rates observed in all-india survey of photovoltaic module reliability 2018. *IEEE J Photovoltaics* 10: 560–567.



AIMS Press

© 2021 the Author(s), licensee AIMS Press. This is an open access article distributed under the terms of the Creative Commons Attribution License (<http://creativecommons.org/licenses/by/4.0>)